**Cimprič Darjan**

SEMINARSKA NALOGA

# Shape memory alloys

Adviser: prof. dr. Janez Dolinšek

13. januar 2007

**Abstract**

The aim of this seminar is an introduction to shape memory alloys, the materials that change shape by applying heat. This paper contents a brief history and a description of general characteristics of the shape memory alloys. At the end are described groups of most widely used commercial applications.

# Contents

# 1 Introduction

Metals are characterized by physical qualities as tensile strength, malleability and conductivity. In the case of shape memory alloys, we can add the anthropomorphic qualities of memory and trainability. Shape memory alloys exhibit what is called the shape memory effect. If such alloys are plastically deformed at one temperature, they will completely recover their original shape on being raised to a higher temperature. In recovering their shape the alloys can produce a displacement or a force as a function of temperature. In many alloys combination of both is possible. We can make metals change shape, change position, pull, compress, expand, bend or turn, with heat as the only activator. Key features of products that possess this shape memory property include: high force during shape change; large movement with small temperature change; a high permanent strength; simple application, because no special tools are required; many possible shapes and configurations; and easy to use - just heat [1]. Because of these properties shape memory alloys are helping to solve a wide variety of problems. In one well–developed application shape memory alloys provide simple and virtually leakproof couplings for pneumatic or hydraulic lines [2]. The alloys have also been exploited in mechanical and electromechanical control systems to provide, for example, a precise mechanical response to small and repeated temperature changes [3]. Shape memory alloys are also used in a wide range of medical and dental applications (healing broken bones, misaligned teeth ...) [2, 4].

# 2 History

First observations of shape memory behaviour were in 1932 by Ölander in his study of "*rubber like effect*" in samples of gold–cadmium [5] and in 1938 by Greninger and Mooradian in their study of brass alloys (copper–zinc) [1, 5]. Many years later (1951) Chang and Read first reported the term "*shape recovery*" [5]. They were also working on gold–cadmium alloys. In 1962 William J. Buehler and his co–workers at the Naval Ordnance Laboratory discovered shape memory effect in an alloy of nickel and titanium. He named it NiTiNOL (for nickel–titanium Naval Ordnance Laboratory) [2, 3].

Buehler's original task was finding a metal with a high melting point and high impact resistant properties for the nose cone of the Navy's missile SUBROC. From among sixty compounds, Buehler selected twelve candidates to measure their impact resistance by hitting them with hammer. He noted that a nickel–titanium alloy seemed to exhibit the greatest resistance to impact in addition to satisfactory properties of elasticity, malleability and fatigue. One day he took some NiTiNOL bars from melting furnace and laid them out on a table to cool. He intentionally dropped one on the floor out of curiosity. The bar produced a bell–like quality sound. Than he ran to the fountain with cold water and chilled the warm bar. The bar was once again dropped on the floor. On his amazement it exhibited the leaden–like acoustic response. Buehler knew that acoustic damping signalled a change in atomic structure that can be turned off and on by simple heating and cooling near room temperature, but he did not yet know that this rearrangement in the atomic structure would lead to shape memory effect [3, 6].

It was in 1960 when Raymond Wiley joined Buehler's research group. He worked on failure analysis of various metals. He demonstrated to his management the fatigue resistance of a NiTiNOL wire by flexing it. The directors who were present at this meeting passed the strip around the table, repeatedly flexing and unflexing it and were impressed with how well it held up. One of them, David Muzzey, decided to see how it would behave under heat. He was a pipe smoker, so he held the compressed NiTiNOL strip in the flame of his lighter. To the great amazement of all, it has stretched out completely. When Buehler heard about that, he realized that it had to be related to the acoustic behaviour he had noted earlier [3, 6]. After this moment, NiTi alloys increased interest of developing applications based on a shape memory alloys.

# 3 Definition of a Shape Memory Alloy

Shape memory alloys are a unique class of metal alloys that can recover apparent permanent strains when they are heated above a certain temperature. The shape memory alloys have two stable phases - the high–temperature phase, called *austenite* (named after English metallurgist

William Chandler Austen [3]) and the low–temperature phase, called *martensite* (named after German metallographer Adolf Martens [3]).
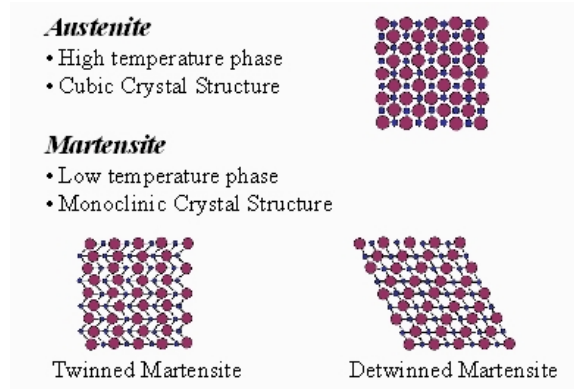


Figure 1: Different phases of a shape memory alloy [8].

The key characteristic of all shape memory alloys is the occurrence of a martensitic phase transformation which is a phase change between two solid phases and involves rearrangement of atoms within the crystal lattice. The martensitic transformation is associated with an inelastic deformation of the crystal lattice with no diffusive process involved. The phase transformation results from a cooperative and collective motion of atoms on distances smaller than the lattice parameters. Martensite plates can grow at speeds which approach that of sound in the metal (up to $1100m/s$). Together with fact, that martensitic transformation can occur at low temperatures where atomic mobility may be very small, results in the absence of diffusion in the martensitic transformation within the time scale of transformation. The absence of diffusion makes the martensitic phase transformation almost instantaneous (a first-order transition). When a shape memory alloy undergoes a martensitic phase transformation, it transforms from its high–symmetry (usually cubic) austenitic phase to a low symmetry martensitic phase (highly twinned monoclinic structure). NiTiNOL's high temperature phase has B2 crystal structure and its low temperature phase has B19' crystal structure. If one ignores the difference between Ni and Ti atoms, B2 crystal structure is simply body–centred cubic and B19 has the same symmetry as hexagonal–close packed, except that the two species of atoms break hexagonal symmetry making the structure to tetragonal. B19' is a small distortion from B19 [7]. See Figure 2.
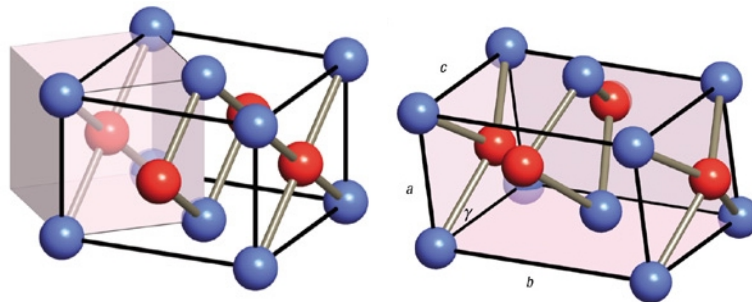


Figure 2: The cubic B2 cell (shaded box) of NiTi (*left*). The distortion to the stress–stabilized B19' structure (*right*). Structural parameters for B2 structure are a = 2.949 Å, b = 4.171 Å, c = 4.171 Å and $\gamma = 90°$; structural parameters for B19' structure are a = 2.861 Å, b = 4.600 Å, c = 3.970 Å and $\gamma = 97.8°$ [9].

A feature of all martensitic transformations is that there are number of equivalent shear directions through which the martensite can form within a region of parent–phase. This results in the formation of martensite variants within the microstructure of a transformed alloy. In Figure

1 at twinned martensite phase, we can see two crystallographically equivalent martensite variants created by different atomic shears from the parent phase. Two opposite shears maintain the macroscopic shape of the crystal block. Such a microstructure, where the shear of one variant is accommodated or "cancelled" by that of the other, is know as a self–accommodated structure. Three–dimensional self–accommodation requires a large number of variants (typically up to 48 in many alloys) [5].

Upon cooling without of applied load the material transforms from austenite into twinned martensite. With heating twinned martensite, a reverse martensitic transformation takes place and as a result the material transforms to austenite. This process is shown in Figure 3. There are four critical temperatures defined. Martensitic start temperature ($M^s$) which is the temperature at which the material starts transforming from austenite to martensite. Second is martensitic finish temperature ($M^f$), at which the transformation is complete and material becomes fully in the martensitic phase. Similar temperatures are defined for reversible transformation. Austenite start temperature ($A^s$) is the temperature at which the reverse transformation starts and austenite finish temperature ($A^f$) at which the reverse transformation is finished and the material is in the austenitic phase.
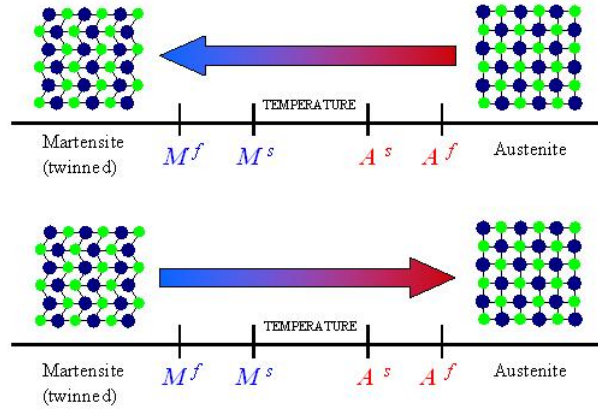


Figure 3: Temperature–induced phase transformation of a shape memory alloy without mechanical loading [8].

We get hysteresis curve for a thermoelastic martensitic transformation as seen on Figure 4. The overall hysteresis between forward and reverse transformation pathways in shape memory alloys is small, typically between 10 and 50 °C [5]. Thermoelastic martensitic transformations form the basis of shape memory alloys behaviour and can be repeated indefinitely as long as high temperature excursions are avoided.
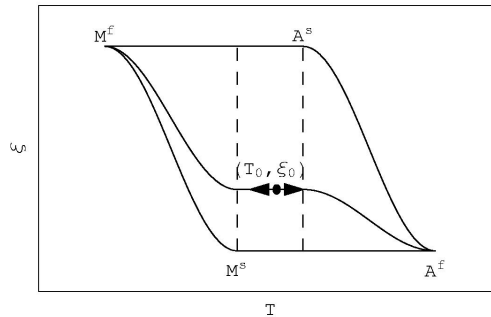


Figure 4: Hysteresis curve for a thermoelastic martensitic transformation. $\xi$ denotes the fraction of martensite in the material. $\xi_0$ and $T_0$ are prescribed initial conditions. They represent a condition that the material contains some martensite ($\xi_0$) and some austenite ($1 - \xi_0$) at a temperature $T_0$.

## 3.1 Mathematical modelling of martensitic transformation

If we denote the fraction of martensite in the material with $\xi$, then at $A^f$ and $M^s$ temperature the value of $\xi$ is 0, and at $M^f$ and $A^s$ temperature the value of $\xi$ is 0. On Figure 4, we can see, how a cosine function may describe the behaviour. Transformation from austenite to martensite ($A \rightarrow M$) can be written as

$$\xi = C_1 \cos \Theta + C_2 = C_1 \cos \alpha_M (T - M^f) + C_2. \tag{1}$$

Initial conditions for austenite to martensite transformation are

$$\xi = 0 \ \text{ at } \ \Theta = \pi \Rightarrow C_1 = C_2, \tag{2}$$

$$\xi = 1 \ \text{ at } \ \Theta = 0 \Rightarrow C_1 = C_2 = \frac{1}{2}. \tag{3}$$

At $M^s$ temperature the material is in austentic phase ($\xi = 0$) thus value of $\Theta$ is $\pi$. We get

$$\Theta = \alpha_M (M^s - M^f) = \pi \ \Rightarrow \ \alpha_M = \frac{\pi}{M^s - M^f}, \ \ M^f \leq T \leq M^s. \tag{4}$$

Similary, the transformation from martensite to austenite ($M \rightarrow A$) can be written as

$$\xi = \frac{1}{2} \cos \alpha_A (T - A^s) + \frac{1}{2}, \tag{5}$$

where

$$\alpha_A = \frac{\pi}{A^f - A^s}, \ \ A^s \leq T \leq A^f. \tag{6}$$

The above transformations and their mathematical representations have basis in initial conditions of material being in fully austenitic or fully martensitic phase. If this process would start at some value $\xi_0$ at a corresponding $T_0$, then the above expressions must be modified. The equations are obtained on the basis that no new martensite is added until the temperature $T$ reaches $M_s$.

Application of the boundary conditions $\xi = \xi_0$ at $\Theta = \pi$ and $\xi = 1$ at $\Theta = 0$ to equation (1) leads to the constants

$$C_1 = \frac{1 - \xi_0}{2}, \tag{7}$$

$$C_2 = \frac{1 + \xi_0}{2}. \tag{8}$$

Transformation from austenite to martensite from initial state $\xi_0$ at $T_0$ can be presented as

$$\xi = \frac{1 - \xi_0}{2} \cos \left( \alpha_M (T - M^f) \right) + \frac{1 + \xi_0}{2}. \tag{9}$$

For transformation from martensite to austenite beginning with $\xi = \xi_0$ and $T = T_0$ on the basis of the assumption that no new austenite is formed until the temperature reaches $A^s$, we can write boundary conditions $\xi = 0$ at $\Theta = \pi$ and $\xi = \xi_0$ at $\Theta = 0$. This gives us

$$C_1 = \frac{\xi_0}{2} = C_2, \tag{10}$$

and therefore,

$$\xi = \frac{\xi_0}{2} \left[ \cos \left( \alpha_A (T - A^s) \right) + 1 \right]. \tag{11}$$

## 3.2 Influence of stress on the characteristic temperatures

Experimental observations indicate that the characteristics temperatures $M^f$, $M^s$, $A^f$ and $A^s$ increase with applied stress as shown in Figure 5. These changes are described by the slopes

$$C_M = \tan \alpha, \tag{12}$$
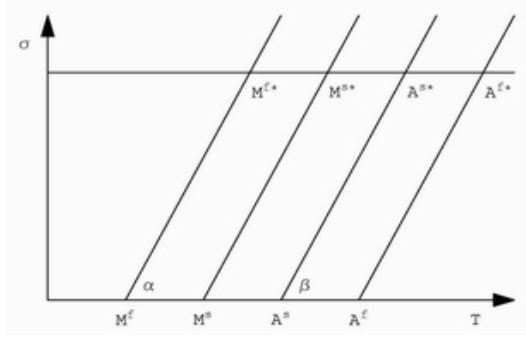
$$C_A = \tan \beta. \tag{13}$$

Figure 5: Influence of stress on critical phase change temperatures.

Generally, it is assumed that $\alpha = \beta$ and $M^f$, $M^s$, $A^f$ and $A^s$ are critical temperatures at which phase changes occur without stress ($\sigma = 0$). With applied external stress ($\sigma \neq 0$), higher temperatures will be needed for a phase change. The increase is linear, with critical temperatures increasing with applied stress. For $M \rightarrow A$ transformation with ($\sigma \neq 0$) we use

$$\xi = \frac{1}{2}\Big[\cos\big[\alpha_A(T - A^s) + b_A\sigma\big] + 1\Big]. \tag{14}$$

This equation reflects an increased temperature proportional to $\sigma$. With reference to Figure 5 we can calculate $b_A$ from conditions $\xi = 0$ at $\sigma \neq 0$ and $T = A^{f*}$,

$$\alpha_A(A^{f*} - A^s) + b_A\sigma = \pi, \tag{15}$$

$$\alpha_A(A^f - A^s + \Delta A^f) + b_A\sigma = \pi. \tag{16}$$

With (6) we get

$$\alpha_A\big(\frac{\pi}{\alpha_A} + \Delta A^f\big) + b_A\sigma = \pi, \tag{17}$$

where $A^{f*} = A^f + \Delta A^f$. Together with $\sigma = \Delta A^f \tan\beta = C_A\Delta A^f$ follows

$$b_A = -\frac{\alpha_A}{C_A}. \tag{18}$$

Similarly,

$$b_M = -\frac{\alpha_M}{C_M}, \tag{19}$$

$$\xi = \frac{1 - \xi_0}{2}\cos\big(\alpha_M(T - M^f) + b_M\sigma\big) + \frac{1 + \xi_0}{2}, \tag{20}$$

for $A \rightarrow M$ transformation. The effect of increased stress is a shift of characteristic to the right (see Figure 6).

Now, we will examine limits of stress. The equation (14) can be written as

$$\xi = \frac{\xi_0}{2}\big[\cos\Theta + 1\big]; \quad \Theta = \alpha_A(T - A^s) + b_A\sigma. \tag{21}$$

Limits of $\Theta$ are

$$0 \leq \Theta \leq \pi. \tag{22}$$

This leads us to

$$0 \leq \alpha_A(T - A^s) + b_A\sigma \leq \pi. \tag{23}$$

From (23) we obtain limits for applied stress $\sigma$ for $M \rightarrow A$ transformation:

$$C_A(T - A^s) - \frac{\pi}{|b_A|} \leq \sigma \leq C_A(T - A^s). \tag{24}$$
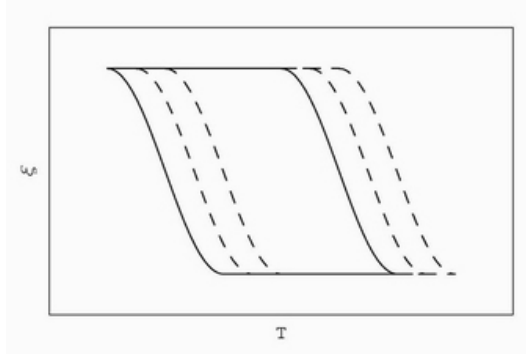
7

Figure 6: Shift of $\xi - T$ characteristic to the right with increased stress (dashing lines).

Fot austenite to martensite transformation the procedure is similar. The result for upper and lower limit od $\sigma$ is

$$C_M(T - M^f) - \frac{\pi}{|b_M|} \leq \sigma \leq C_M(T - M^f). \tag{25}$$

Using definitions (4), (6), (18) and (19) above limits are simplified:

$$C_A(T - A^f) \leq \sigma \leq C_A(T - A^s), \tag{26}$$

$$C_M(T - M^s) \leq \sigma \leq C_M(T - M^f). \tag{27}$$

The lower limit of (27) for $\sigma$ represents the limit above which a fully austenite wire will begin to experience martensitic phase. This is also the limit of linearity for the stress above which the stress–strain relationship will be nonlinear because of nonzero martensite.

## 3.3 Thermodynamic aspect on martensitic transformation

Transformation temperatures ($M^s$, $M^f$, $A^s$, $A^f$) can be determined by measuring some physical properties as a function of temperature, since many physical properties often drastically change upon starting or finishing martensitic transformation (see Figure 7).
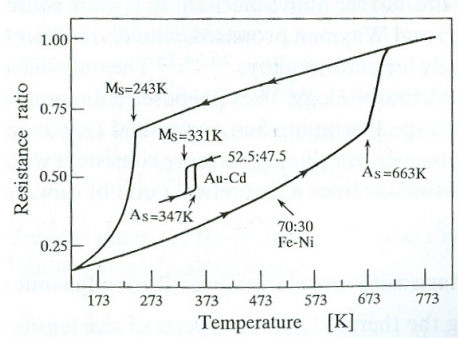


Figure 7: Electrical resistance changes during cooling and heating Fe–Ni and Au–Cd alloys, illustrating the hysteresis of the martensitic transformation on cooling, and reverse transformation on heating, for non–thermoelastic and thermoelastic transformations respectively [10].

Since the martensitic transformations are not associated with a compositional change, the free energy curves of both parent and martensite phases as a function of temperature may be represented as schematically shown in Figure 8, where $T_0$ represents the thermodynamic equilibrium temperature between the two phases, and $\Delta G^{p \to m}|_{M^s} = G^m - G^p$ represents the driving force for the nucleation of martensite, where $G^m$ and $G^p$ represent the Gibbs free energy of martensite and austenite. The same argument applies for the reverse transformation. Thus, $T_0$ was approximated

8

by $\frac{1}{2}(M^s + A^s)$. A Gibbs free energy change of a system upon martensitic transformation may be written as follows

$$\Delta G = \Delta G_c + \Delta G_s + \Delta G_e = \Delta G_c + \Delta G_{nc},$$

where $\Delta G_c$ is a chemical energy term originating in the structural change from parent to martensite, $\Delta G_s$ is a surface energy term between parent and martensite, $\Delta G_e$ is an elastic (pluc plastic in the non–thermoelastic case) energy term around the martensite, and $\Delta G_{nc}$ is a non–chemical energy term. In most martensitic transformations, $\Delta G_{nc}$ is equallay as large as $\Delta G_c$, which is an essential point when we discuss martensitic transformations. Because of this, supercooling of $\Delta T_s$ is necessary for the nucleation of a martensite, and superheating is necessary for the reverse transformation [10]. By the same token, $M^s$ is not the same as $M^f$, since the elastic energy around the martensite resists the growth of the martensite unless a further driving force is given (i.e. cooling) [10].
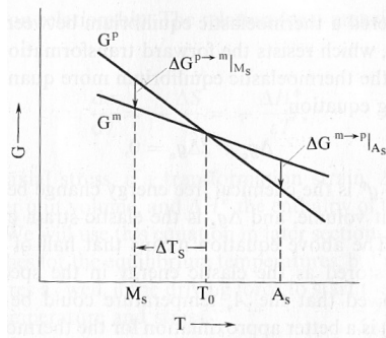


Figure 8: Schematic representation of free energy curves for both parent and martensitic phases, and their relation to the $M^s$ and $A^s$ temperatures. $\Delta T_s$ is the supercooling required for the transformation [10].

When we discuss martensitic transformations, we classify them into two categories, thermoelastic and non–thermoelastic. These are shown in Figure 7. In the case of the Au–Cd alloy, the transformation hysteresis is as small as $15K$, while in Fe–Ni alloy. it is as large as $\sim 400K$. In first case, the driving force for the transformation is very small (as evidenced by the small temperature hysteresis), the interface between austenite and martensite is very mobile upon cooling and heating, and the transformationis crystallographically reversible in the sense that the martensite reverts to the parent phase in the original orientation. This type of transformation is called thermoelastic. In second case, the driving force is very large, the interface between austenite and martensiteis immobile once the martensite grows to some critical size, and the reverse transformation occurs by the renucleation of the parent phase, and thus the transformation is not reversible. It is known that shape memory effect and superelasticity are generally charachteristic of thermoelastic transformations [10].

Originally the notion of the thermoelastic transformation was introduced by Kurdjumov and Khandros, who observed the growth and shrinkage of a martensite plate upon cooling and heating respectively in a Cu–Al–Ni alloy [10]. They considered a thermoelastic equilibrium between chemical energy and elastic energy, which resists the forward transformation. Olson and Cohen considered the thermoelsatic equilibrium more quantitatively, and derived the following equation

$$\Delta g_c + 2\Delta g_e = 0,$$

where $\Delta g_c = g^m - g^p$ is the chemical free energy change between parent and martensite per unit volume, and $\Delta g_e$ is the elastic strain energy around the martensite plate [10]. The above equation means, that half of the chemical free energy change is stored as the elastic energy in the specimen. From this analysis, they showed that the $A^s$ temperature could be below $T_0$. Tong and Waymann proposed that

$$T_0 = \frac{1}{2}(M^s + A^f)$$

is a better approximation for the thermoelastic transformation [10].

9

# 4 One–way memory effect

## 4.1 Macroscopic range

If an alloy, which is in a state of self–accommodated martensite, is deformed by applying mechanical load and then unloaded, remains deformed. If the alloy is then reheated to a temperature above the austenite finish temperature, it recovers original macroscopic shape. This is so–called one–way memory effect (see Figure 9). As long as the total strain does not induce permanent plastic flow, deformation may be of any type (e.g. tension, compression, bending or more complex combinations) [3].
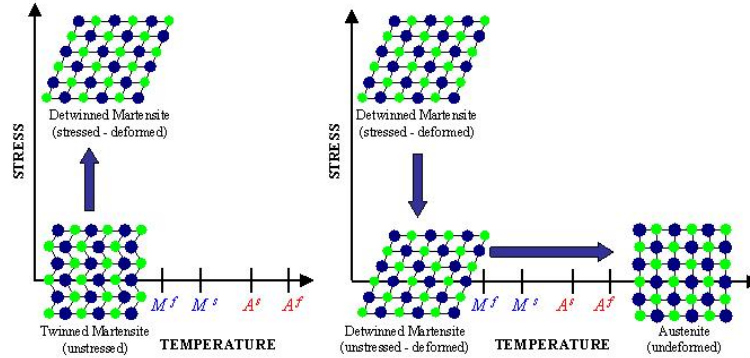


Figure 9: One–way shape memory effect [8].

## 4.2 Microscopic range

During the one–way memory effect internal structural changes take place. When we apply load to the self–accommodated martensite, this structure becomes deformed through variant rearrangement, resulting in a net macroscopic shape change. When the alloy is unloaded this deformed structure remains, resulting in an apparent permanent strain. If the alloy is now reheated to a temperature above the martensitic transformation range the original parent phase microstructure and macroscopic geometry is restored. This is possible because no matter what the post–deformation distribution of martensite variants, there is only one reversion pathway to parent phase for each variant [5]. If the alloy is cooled again under martensitic finish temperature, a self–accommodated martensite microstructure is formed and the original shape before deformation is retained. Thus one–way shape memory is achieved. The maximum strain recovered through this process depends on the shape memory system. Typically longitudinal strain is in the range of 1 to 7 %, in some cases up to 10 % [3, 5].
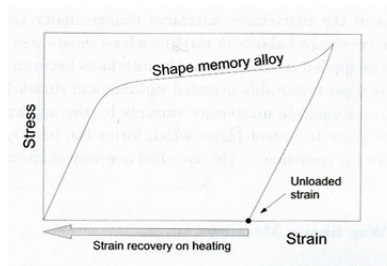


Figure 10: Stress-strain behaviour during the one–way memory effect [5].

### 4.2.1 Martensite variants growth

In the shape memory alloys the interfaces between martensite variants are mobile and their positions can be influenced by external variables. Probably most important is applied stress. The herringbone structure of martensites essentially consists of twin-related, self-accommodating variants. The shape change among the variants tends to cause them to eliminate each other. As a result, little macroscopic strain is generated (Figure 11b). The positions of the martensite interfaces change under the influence of stress, creating a balance of variants whose shears best accommodate the direction of applied strain. The interfaces between variants move to "grow" the most favourably oriented variants and shrink the least favourably oriented. Some variants become dominant in the configuration (Figure 11c). This process creates a macroscopic strain, which is recoverable as the crystal structure reverts to austenite during reverse transformation [2, 5, 11].
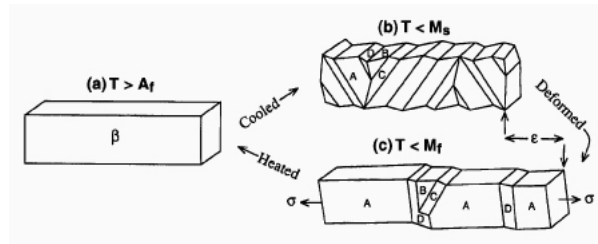


Figure 11: (a) Parent phase of a crystal. (b) Self–accommodating twin–related variants after cooling and transformation to martensite. (c) Variant A becomes dominant when stress is applied. Upon heating, the material reverts to the beta phase and recovers its original shape [11].
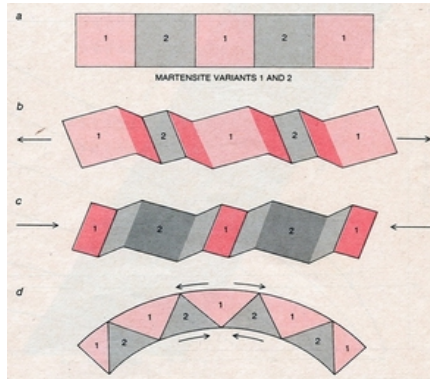


Figure 12: Martensite variants grow at different rates when they are subjected to stress. Here is an example of only two variants. In the absence of stress (a) plates of the two variants develop with equal probability. If the material is subjected to tensile stress (b), plates of variant 1 grow at the expense of those of variant 2. If the material is subjected to compression (c), the preference is reversed: variant 2 grows at the expense of variant 1. If the material is bent (d), the variants grow according to whether the crystals are locally under tension or compression [2].
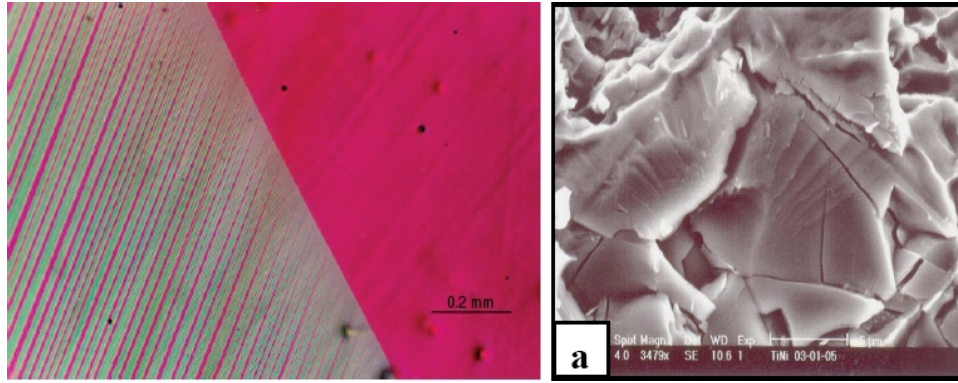
Figure 13: (*left*) Microstructure of twinned martensite meeting a homogeneous region of austenite in a Cu-Al-Ni alloy [12]. (*right*) Scanning electron micrograph of $Ti_{51}Ni_{49}$ alloy showing an average grain size of approximately $20\mu m$ [13].

# 5  Two–way memory effect

In one–way memory effect there is only one shape "remembered" by the alloy. That is the parent phase shape (so-called hot shape). Shape memory alloys can be processed to remember both hot and cold shapes. They can be cycled between two different shapes without the need of external stress.
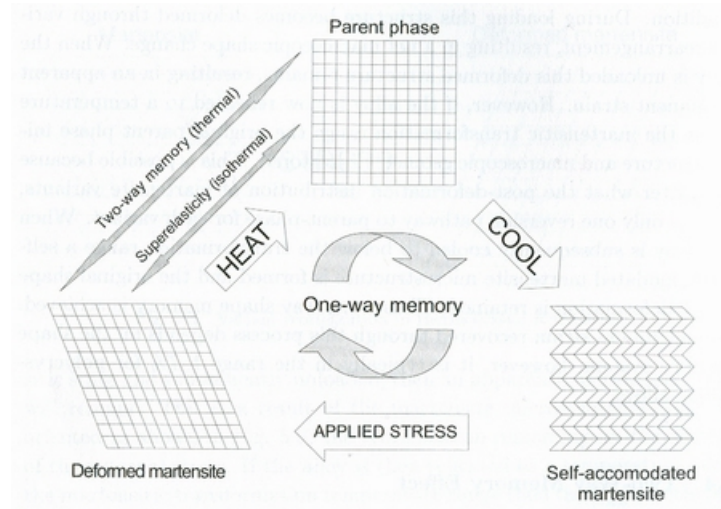


Figure 14: Microstructural changes during thermal memory and superelastic phenomena [5].

Two–way shape memory changes rely entirely on microstructural changes during martensitic transformation which occur under the influence of internal stress. Self–accommodation of the martensite microstructure is lost in the two–way effect due to the presence of these internal stresses. Predominant variants are formed during transformation (i.e. there is an excess of certain variants within the martensite microstructure compared to self–accommodated structures.) [5, 8]. This results in achieving deformed martensite phase directly by cooling parent phase under the influence of internal stress. Internal stress may be introduced in a number of ways. Usually we talk about "training" of shape memory alloy. Internal stress must be stable on thermal cycling through the transformation. Internal stress is usually a result of irreversible defects. After each loading–unloading cycle, a small residual strain remains. Irreversible defects can also be created through the presence of particles. Two of the most common training methods create two–way memory through the introduction of dislocation arrays and are achieved by [5]:

- Cyclic deformation at a temperature below $M^f$ followed by constrained heating in the cold–shape to a temperature above $A^f$.

- Cyclic deformation between the hot and cold–shapes at a temperature above $A^f$.

# 6    Pseudoelasticity or the superelastic effect

It is also possible to induce a phase transformation by applying a pure mechanical load isothermally at a temperature above austenite finish temperature. The result of this load application is fully detwinned martensite and very large strains are observed. The martensite formed in this way is known as stress–induced martensite and is only stable under the application of stress. On unloading, the reduction in stress and surrounding elastic forces generated during transformation cause the martensite to shrink back to the original parent phase. This effect is known as *pseudoelastic* or *superelastic effect* [5, 8]. Figure 15 shows the mechanical behaviour of such superelastic material, and compares it to a conventional metallic alloy. Such superelastic materials can fully recover deformations up to 6-7 % strain, depending on alloy type.
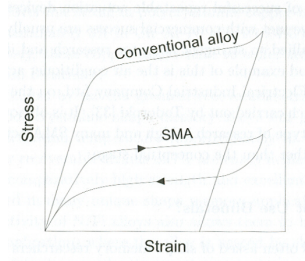


Figure 15: Comparison of the stress–strain curves of conventional and superelastic alloys [5].

# 7    Commercial shape memory alloys

Despite of growing list of alloys that display shape memory effect only two alloy systems have achieved any level of commercial exploitation. These are NiTi (nickel–titanium) and copper–based alloys. Properties of both systems are quite different. The NiTi alloys have greater shape memory strain (up to 8 % versus 4–5% for the copper–based alloys), tend to be much more thermally stable, have excellent corrosion resistance and have much higher ductility. On the other hand, the copper–based alloys are much less expensive, exhibit higher actuation temperatures (approximately in the range -200 to +200 °C) than NiTi alloys and are sometimes the only choice for high temperature applications (i.e. above 100 °C). Unfortunately, these copper–based alloys tend to suffer from low strength and poor corrosion resistance [5, 11].

## 7.1    Nickel–titanium shape memory alloys

Nickel–titanium alloys have far greatest recoverable strains of commercially available shape memory alloys. Fully recoverable strains of 7% are easily achieved with these alloys. The temperature at which the phase change associated with the memory effect takes place can be adjusted from $-200$ °C to $+100$ °C by altering the propositions of nickel and titanium around the equi–atomic ratio of 50 % nickel and 50 % titanium. Differences of just 0.1 atomic percent can easily change transformation temperatures by 20 °C or more [2, 5]. For this reason production and processing of NiTi alloys must be very strictly controlled. The manufacture of NiTi alloys follows closely the procedures of conventional titanium alloy manufacture. Because titanium easily forms oxides, carbides and nitrides a vacuum melting process is essential. This ensures good homogeneity of the alloy, and enables transformation temperatures to be controlled to within 5 °C [2, 5, 11]. Because of this careful fabrication and often small production are NiTi alloys rather expensive.

The greatest benefit of NiTi alloys over other commercial shape memory alloys is it's excellent corrosion resistance. The passive titanium dioxide ($TiO_2$) surface film results in a corrosion resistance comparable to 316L stainless steel. Formation of this film is exactly the same as for pure titanium. The film is very stable and resistant to many forms of potentially corrosive attack [5]. NiTi's corrosion resistance has lead to studies on bio–compatibility of these alloys and a number of medical applications. Result of studies was that bio-compatibility is excellent [1, 2, 5, 17]. Organs are showing no signs of metallic contamination. It is thought that the titanium–rich oxide surface prevents nickel (potentially harmful) coming in touch with tissue. This has resulted in a great research activity of NiTi alloys in medicine.
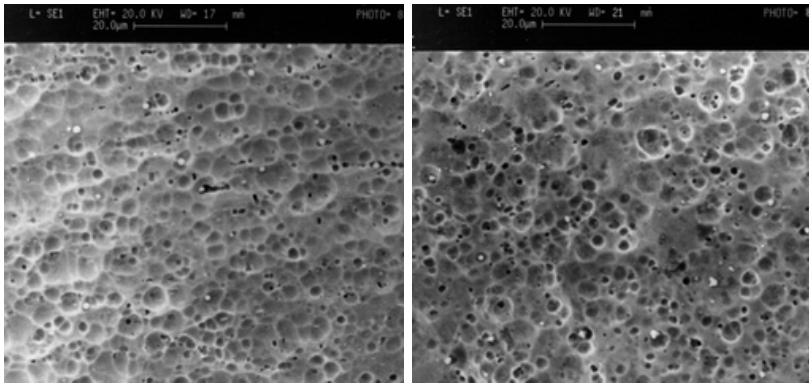


Figure 16: The surface of NiTi clamp before implantion (*left*) and after 17 months exposure in the human body (*right*). There is no trace of corrosion visible. Porosity can be neglected on this scale ($\approx 10\mu m$). [17].

## 7.2 Copper–based shape memory alloys

Brass (copper–zinc) has been known to have a shape memory since 1930's [2]. These alloys are based on between 68 and 80 % copper. The remaining 20 to 32 % consists of zinc and aluminium in various proportions. Slight shifts in composition rise or lower critical temperatures in range from $-200\,°C$ to $+200\,°C$ (see Figure 17) [11]. At higher temperatures there is a tendency for martensite to become unstable, so the usual upper temperature for transformation is around $+150\,°C$ [11]. They have maximum recoverable strain of approximately 5% [5].

Copper–based shape memory alloys have the advantage that they are made from relatively cheap materials using conventional metallurgical processes such as induction melting. Nitrogen or other inert gases should be used for shielding purposes over the melt and during pouring to prevent zinc evaporation. The handicap of these shape memory alloys is that martensitic phase is stabilised by long term ageing at room temperatures. This causes an increase in transformation temperature over time [1, 11].

Usually small quantities of boron, cerium, cobalt, iron, titanium, vanadium and zirconium (less than 1%) are added to control grain size to about $50 - 100\mu m$ [14]. Without the addition of grain growth control additives, the grain size of these alloys can be quite large (in the order of mm) [14]. This leads to brittleness, because grain boundaries become large and an alloy can easily crack. Additions should be made carefully as they can upset the stability of the structure, which affects the shape memory characteristics [11].
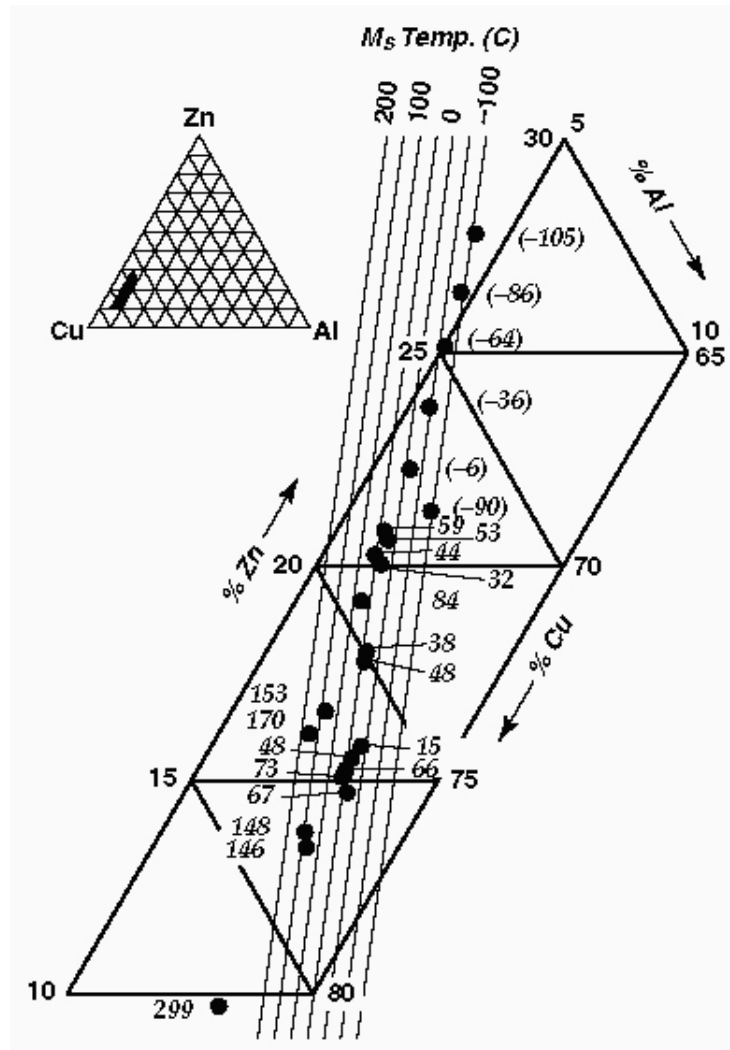
Figure 17: Martensite formation temperatures, $M^s$, for ternary (three–element) alloys of copper, zinc and aluminium can be made to vary over more than $400\,^\circ$C as a result of only small changes in composition. The shape memory alloys all lie in the copper–rich corner of the triangle representing ternary mixtures. The amount of aluminium varies from about 4 to 10%, the amount of zinc from just under 10 to 28 % [11].

# 8 Applications of shape memory alloys

Shape memory alloys have wide range of use. That is why categories of application have been introduced [5, 11, 17].

## 8.1 Free recovery

This category of shape memory alloys is deformed while in a martensitic phase. The only function required is that they return to previous (parent) shape upon heating. A prime application is a blood–clot filter. The filters are constructed from NiTi wires and are used in one of the outer hearth chambers to trap blood clots, which potentially could cause serious health problems if travelling around the blood circulation system. The blood–clot filter is introduced in a compact cylindrical form about 2.0-2.5 mm in diameter. The body heat causes transformation to its functional shape. The wire is shaped to anchor itself in a vein and catch passing clots [5, 15].
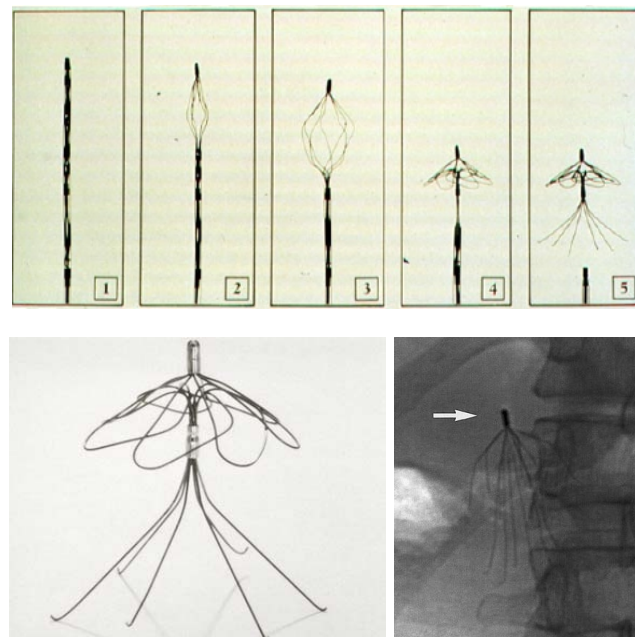


Figure 18: The blood–clot filter [15].

## 8.2 Constrained recovery

The alloy is prevented from full shape recovery. This means that the alloy generates stress on the constraining element. The most successful example of this type of product are hydraulic–tube couplings. This kind of couplings was on the first place made for F–14 jet fighter [1, 2]. Coupling is machined at normal temperature to have inner diameter 4 % less than the outer diameter of the tubes to be joined. After cooling the coupling under the $M^f$ temperature, the diameters are expanded to have greater diameter than the tubes (see Figure 19 *top*). When the coupling is warmed to austenite phase, it shrinks in diameter and strongly holds the tube end together (see Figure 19 *bottom*). The tubes prevent the coupling to recover its original shape. This creates stresses powerful enough to create a joint, which is better than a weld.
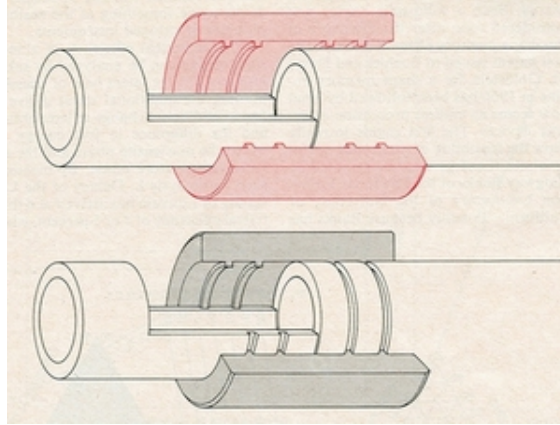
Figure 19: Hydraulic–tube couplings. First couplings were made for F–14 jet fighter from Ni–Ti alloy, now are usually made from Cu-Zn-Al alloy.[2].

## 8.3 Actuation recovery

The alloy is able to recover its shape but operates against applied stress, resulting in work production. One application of this group is a temperature–actuated switch. The switch can be designed so that it opens or closes above particular temperature (see Figure 20). Those switches are usually applied in instruments for safety purposes. One such example is a fire safety switch, which is designed to shut off the electricity or flammable gas flow when fire occurs [2, 5].



Figure 20: Temperature–actuated switch. If the switch is designed to close above the $A^f$ temperature (*top*), a straight rod of alloy in initial shape is cooled to martensite phase (*red colour*). Then an alloy is reshaped under stress. When the rod is heated above $A^f$ temperature, the martensite disappears and the rod straightens, closing the switch. If the switch is designed to open above $A^f$ temperature, the rod must be bent before cooling (*bottom*). The rod is then straightened out before it is placed in the switch [2].

## 8.4 Superelastic recovery

The only isothermal application of the memory effect, superelastic recovery involves the storage of potential energy through comparatively large but recoverable strains. This is commercially used in orthodontic applications, especially in correcting misaligned teeth. Superelastic NiTi wires are used for making continuous, gentle, corrective force to give large rapid movement of teeth. Based

on clinical observations the optimal forces for tooth movement are $0.5 - 1.25N$ [16]. The forces at the lower end of the range correspond to the smaller rooted teeth and the forces at the upper end of range are optimal for the larger rooted teeth. Optimal wires are from NiTi alloy with diameter from 0.4 mm to 0.6 mm [16]. Similar shape memory alloy devices are used for healing broken bones. Staples of the shape memory materials are attached to each part of broken bone. These staples apply a constant, well–defined force to pull the two pieces together. This force helps to heal up the two pieces of bone together [1, 4, 17].
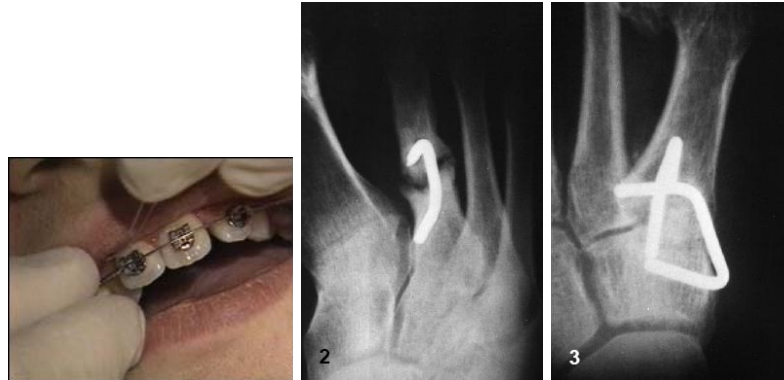


Figure 21: Arch wires for orthodontic correction of misaligned teeth (*left*) and TiNi shape memory clamps for healing broken bones (*middle, right*) [17].

# 9    Conclusion

This seminar has presented basic facts about shape memory alloys and some of the most common used applications. The most wide–spread usage of shape memory alloys is for medical purposes, and this market is still growing. Medical industry has developed a number of products using NiTi alloys because of their excellent biocompatibility and large pseudoelasticity. Many more of these applications are likely.

The potential for use in engineering structures is limited by the range of temperatures within which phase change may take place and the rapidity with which these changes occur. The area of thermal shape change that perhaps has the greatest potential is that of actuation. Many patents exist based on the principle of using shape memory alloy element as a thermal actuator which converts thermal energy into mechanical work. Research groups are trying to improve properties of these alloys or finding alloys with better properties. Recent interest in the development is concentrated on iron-based alloys.

Described metals are not only materials which posses shape memory effect. A group of scientists has discovered a plastic that changes shape by applying light. With this discovery new possible applications were introduced (i.e. photosensitive switch) [18].

# A  Physical and mechanical properties of shape memory alloys

| | NiTi | Cu-based Alloys |
|---|---|---|
| Density $[g/cm^3]$ | $6.4 - 6.5$ | $7.1 - 8.0$ |
| Melting point $[°C]$ | 1250 | $950 - 1050$ |
| Thermal conductivity $[W/mK]$ | | |
| *martensite* | $8.6 - 10.0$ | $-$ |
| *parent phase* | 18 | $79 - 120$ |
| Electrical resistivity $[\times 10^{-6}\Omega m]$ | | |
| *martensite* | $0.5 - 0.6$ | 0.14 |
| *parent phase* | $0.82 - 1.1$ | 0.07 |
| Co. thermal expansion $[\times 10^{-6}K^{-1}]$ | | |
| *martensite* | 6.6 | $16. - 18.0$ |
| *parent phase* | $10.0 - 11.0$ | $-$ |
| Specific heat capacity $[J/kgK]$ | $470 - 620$ | $390 - 440$ |
| Enthalpy of transformation $[J/kg]$ | $19.0 - 28.0$ | $7.0 - 9.0$ |
| Transformation temperature range $[°C]$ | $-200 - 120$ | $-200 - +200$ |
| Corrosion performance | Excellent | Poor |
| Bio–coompatibility | Excellent | Assumed poor |

Table 1: Physical properties of shape memory alloys [5].

| | NiTi | Cu-based Alloys |
|---|---|---|
| Young's modulus $[\times 10^9 N/m^2]$ | | |
| *martensite* | $28 - 41$ | 70 |
| *parent phase* | $70 - 97$ | $70 - 100$ |
| Yield strength $[\times 10^6 N/m^2]$ | | |
| *martensite* | $70 - 140$ | $80 - 300$ |
| *parent phase* | $195 - 690$ | $150 - 350$ |
| Ultimate tensile strength $[\times 10^6 N/m^2]$ | | |
| *martensite* | 895 | 400 |
| *parent phase* | 1900 | 1000 |
| Elongation at failure $[\%]$ | | |
| *Fully annealed* | $25 - 50$ | $8 - 15$ |
| *Work hardened* | $5 - 10$ | $8 - 15$ |
| Hot workability | Poor-fair | Very good |
| Cold workability | Poor | Good |
| Machinability | Poor | Very good |

Table 2: Mechanical properties of shape memory alloys [5].

# References

[1] "Shape-Memory Alloys – Metallurgical Solution Looking for a Problem", *Metallurgia*, Vol. 51, No. 1, January 1984, pp. 26–29

[2] Schetky L. M., "Shape-Memory Alloys", *Scientific American*, Vol. 241, No. 5, November 1979, pp. 74–82

[3] Srinivasan A. V., McFarland Michel D., *Smart structures – analysis and design*, Cambridge university press (2001), pp. 26–69

[4] Anson T., "Shape Memory Alloys - Medical Applications", *Materials World*, Vol. 7, No. 12, December 1999, pp. 745–747

[5] Worden K. Bullough W. A., Haywood J., *Smart technologies*, World Scientific (2003), pp. 109–135

[6] Kauffman G. B., Mayo I., "The Story of Nitinol: The Serendipitous Discovery of the Memory Metal and Its Aplications", *The Chemical Educator*, Vol. 2, No. 2, 1996

[7] Ackland G. J., "Atomistic modelling of the Shape Memory Effect", eprint arXiv:cond-mat/0509456, September 2005

[8] Texas A&M Smart Lab, "Introduction to Shape Memory Alloys", http://smart.tamu.edu/overview/overview.html

[9] Huang X., Ackland G. J., Rabe K. M., "Crystal structures and shape–memory behaviour of NiTi", *Nature Materials*, No. 2, 2003, pp. 307-311

[10] Otsuka K., Wayman C. M., *Shape memory materials*, Cambridge university press (1998), pp. 21–25

[11] Hodgson D. E. , *Shape Memory Applications, Inc.*, Wu M. H., *Memry Technologies*, and Biermann R. J., *Harrison Alloys, Inc.*, http://web.archive.org/web/20030605085042/http://www.sma-inc.com/SMAPaper.html

[12] Cui J., Chu Y. S., Famodu O. O., Furuya Y., Hattrick-Simpers J., James R. D., Ludwig A., Thienhaus S., Wuttig M., Zhang Z., Takeuchi I., "Combinatorial search of thermoelastic shape–memory alloys with extremely small hysteresis width", *Nature materials*, Vol. 5, April 2006, pp.286–290

[13] Yadav T. P., Durgesh R. K., Subrahmanyam V. S., Srivastava O. N., "Effect of the Fe substitution in Ti–Ni shape memory alloys", http://arxiv.org/abs/cond-mat/0610340

[14] Van Humbeeck J., Cederstrom J., "The present state of shape memory materials and barriers still to be overcome", *The first international conference on shape memory and superelastic technologies*, March 1994, pp. 1–6

[15] Murray R., "Initial Experience in Humans with a New Retrievable Inferior Vena Cava Filter", *Radiology*, Vol. 225, September 2002, pp. 835–844

[16] Finander B. V., Liu Y., "Characterization of the unloading forces of Ni–Ti orthodontic archwires", *The first international conference on shape memory and superelastic technologies*, March 1994, pp. 151–156

[17] Musialek J., Filip P., Nieslanik J., "Titanium-nickel shape memory clamps in small bone surgery", *Journal Archives of Orthopaedic and Trauma Surgery*, Vol. 117, No. 6–7, July 1998, pp. 341–344

[18] Thomson E. A., "Intelligent plastics change shape with light", *MIT Tech Talk*, Vol. 49, No. 25, April 2005, pp. 5